URTeC: 608

Optimizing Completions in Tank Style Development

Peter Kaufman*[1], Mark McClure[2], Nick Franciose[1], Sean Owens[1], Fabiano Srur[1], David Russell[1]. [1]QEP Resources, Inc. [2]ResFrac Corporation.

Copyright 2019, Unconventional Resources Technology Conference (URTeC) DOI 10.15530/urtec-2019-608

This paper was prepared for presentation at the Unconventional Resources Technology Conference held in Denver, Colorado, USA, 22-24 July 2019.

The URTeC Technical Program Committee accepted this presentation on the basis of information contained in an abstract submitted by the author(s). The contents of this paper have not been reviewed by URTeC and URTeC does not warrant the accuracy, reliability, or timeliness of any information herein. All information is the responsibility of, and, is subject to corrections by the author(s). Any person or entity that relies on any information obtained from this paper does so at their own risk. The information herein does not necessarily reflect any position of URTeC. Any reproduction, distribution, or storage of any part of this paper by anyone other than the author without the written consent of URTeC is prohibited.

Abstract

Tank-style development in the thick Spraberry-Wolfcamp sequence in the Midland Basin offers a variety of operational efficiency gains which directly translate into cost savings for the operator who has the foresight to plan their acreage development in this manner. Simultaneous development of multiple stacked pay zones presents a technical challenge to maximize production from each zone and the value of the entire DSU, while achieving cost savings, as appropriate. Optimizing completions in tank-style development in a multi-zone pay system is conducted through a combination of well experiments, field trials, and numerical modeling. Using longer stages allows an operator to increase the pace at which wells are completed and translates directly into cost savings. Completing two wells at once further accelerates development, but surface equipment capabilities must be considered if maximum pump rate per well is restricted. Balancing this reduced pump rate with limited-entry can be used to maximize cluster efficiency and the likelihood that hydraulic fractures propagate from each perforation cluster in a stage. Data from RA tracers and step-down tests show the effectiveness of limited-entry on maximizing cluster efficiency. Hydraulic fracture modeling provides insight into the development of competing fractures during the completions operations. Field observations from RA tracers and step-down tests show that the limited-entry approach of reducing shots-per-foot and perforation diameter and focusing on perforation friction pressure instead of total rate leads to equally effective stimulation in a more operationally efficient manner. Hydraulic fracture modeling supports how limited-entry can be used to effectively stimulate longer stages and complete at lower pump rates by optimizing perforation friction pressure. Hydraulic fracture modeling also shows the impact of stress shadowing on hydraulic fracture geometry of different designs in stacked field development. Forward modeling of production from the hydraulic fracture models allows quantification of the value of the operational efficiency gains. This work will highlight how one operator worked to balance optimal fracture design with operational efficiency to maximize the value of a DSU in a stacked, tank-style development. This presentation integrates field and well level completion results, historical stage-level data analytics, and forward modeling of hydraulic fracturing and production in a coupled numerical simulator.

Introduction

Tank-style development in the thick Spraberry-Wolfcamp sequence in the Midland Basin offers a variety of operational efficiency gains which directly translate into cost savings for the operator who has the

foresight to plan their acreage development in this manner (Thompson et al., 2018). Simultaneous development of multiple stacked pay zones presents a technical challenge to maximize production from each zone and the value of the entire DSU, while achieving cost savings, as appropriate. Figure 1 shows a typical one-mile wide DSU which is being developed from left to right using a tank-style approach. Pod 5 is currently drilling, with pod 4 serving as a drilling buffer between it and the completions operations in pod 3. Pod 2 is already completed, but has not been put on production to maintain a pressure wall between the completing wells and production in pod 1. As drilling and completion are finished on their respective pods, the tank development marches to the right, with drilling moving to pod 6, completions moving to pod 4, and production initiated in pod 2.

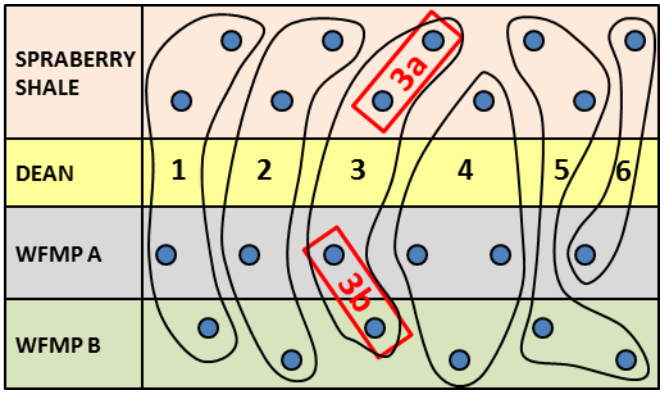

Figure 1. Schematic block diagram for a typical one-mile DSU with grouped well pods designated 1-6.

While there are many metrics to evaluate completion improvement, increasing the pace at which wells are completed results in cost savings from reduced crew and equipment time as well as accelerating the pace at which wells are brought to production. Figure 2 shows the improvements in completion pace realized during 2018 as a result of using longer stages, pairing more wells for simultaneous fracturing, and gaining overall operational efficiency. Using longer stages clearly allows an operator to increase the pace at which wells are completed and translates directly into cost savings. Completing two wells at once further accelerates development, but surface equipment capabilities must be considered if maximum pump rate per well is restricted.

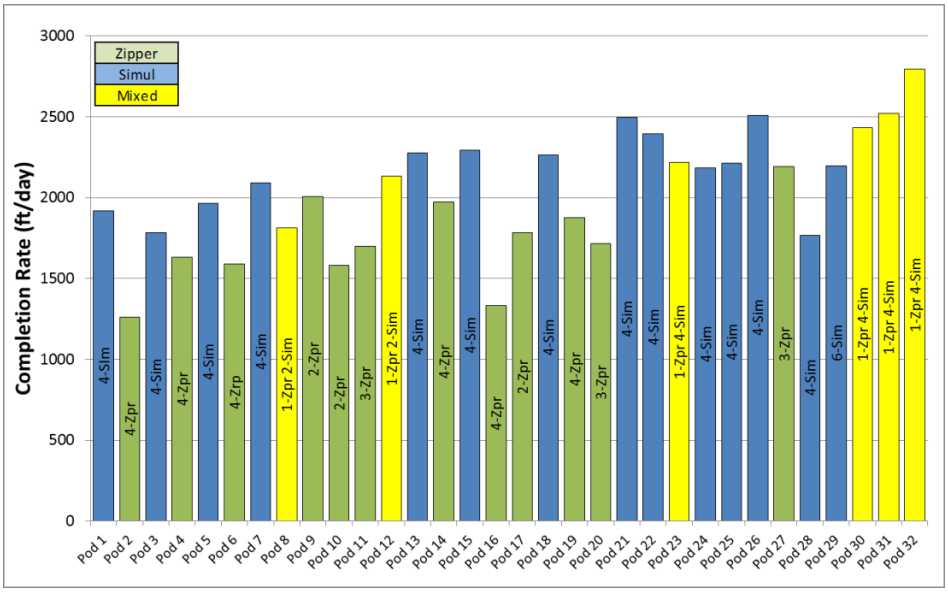

Figure 2. Completion rate improvements during 2018.

While it is critical that improvements in completion efficiency do not come at the expense of production, because of the considerable delay between operational changes and meaningful production metrics (e.g., best six months oil production), it is possible that design changes inadvertently result in poorer outcomes. For this reason, a combination of completion diagnostics, fundamental physical relationships, and numerical modeling are used to guide completion optimization.

For example, employing longer stages while maintaining or decreasing cluster spacing results in more clusters per stage. Simultaneous completion reduces pump rate per well. These two factors together decrease the pump rate per cluster, which could have a detrimental effect on created surface area. To balance this lower rate per cluster, limited-entry and extreme limited entry can be used to maximize cluster efficiency and the likelihood that hydraulic fractures propagate from each perforation cluster in a stage (Cramer, 1987; Weddle et al., 2018).

Theory and Methods

Field data

Radioactive tracers were pumped on both a Spraberry and a Wolfcamp well to evaluate the effectiveness of a limited-entry design at a rate of at least 2.5 BPM per perforation and about 1000 psi total perforation friction. In both wells, ten longer stages with 15 perforation clusters were traced. Review of the tracer data indicated that 97% and 94% of the clusters in the Spraberry and Wolfcamp wells, respectively, were activated. Figure 3 shows an example of a traced stage with good proppant coverage across all 15 clusters.

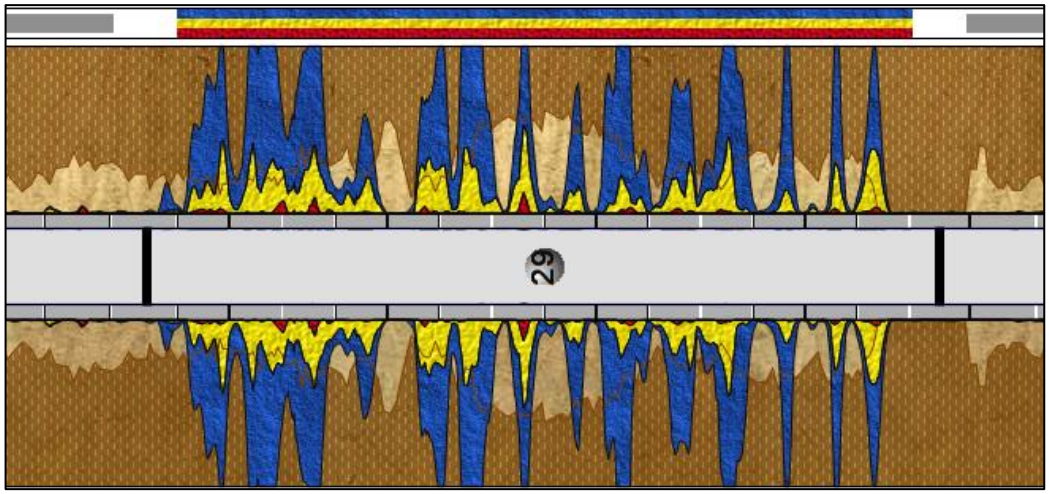

Figure 3. Radioactive tracer log for one stage with clusters, showing well distributed proppant across all clusters.

Step-down test results were compiled for 30 stages in six different Spraberry and Wolfcamp wells with stages designed to achieve at least 2.5 BPM per perforation. These included wells with longer stages, higher maximum rates, and more clusters and wells with shorter stages, lower maximum rates, and fewer clusters. Results are summarized on Table 1. Median total perforation efficiency exceeded 80% for both Spraberry and Wolfcamp zones, demonstrating that the majority of holes, and consequently perforation clusters, were active.

	Spraberry Shale	Wolfcamp
Number of Step-down Tests	20	10
Median number of open perforations	84%	80%
Tortuosity (psi/sqrt(BPM))	78	83

Table 1. Summary of step-down tests for limited-entry designs

Hydraulic fracture modeling supports how limited-entry can be used to effectively stimulate longer stages and complete at lower pump rates by maximizing the designed perforation friction pressure. Hydraulic fracture modeling also shows the impact of stress shadowing on hydraulic fracture geometry for different designs in stacked field development. Forward modeling of production from the hydraulic fracture models allows quantification of the value of the operational efficiency gains.

Numerical simulation approach

Simulations are performed with ResFrac, a combined hydraulic fracturing, wellbore, and reservoir simulator. McClure and Kang (2018) provide a detailed technical description. The approach is briefly summarized in this section.

Mass balance equations are solved for fluid components (water, oil, and gas in the black oil model), water solute components (such as high viscosity friction reducer), and proppants. Mechanical equilibrium equations are solved to calculate stress shadow from fracture opening and propagation and from fluid pressure changes in the matrix. Fracture stress shadow is calculated with the 3D displacement discontinuity method. All equations are solved in a fully coupled approach; all governing equations are satisfied in every element in every timestep. The hydraulic fractures are meshed as cracks with aperture on the order of millimeters, and the cubic law is used to calculate conductivity. Proppant transport is described with a detailed treatment that considers gravitational settling, gravitational convection, hindered settling, bed slumping, and other effects. As proppant concentration within a fracture approaches 0.66 (volume of proppant/volume of fracture), the proppant becomes immobilized into a packed bed of particles, and the fluid flow equations transition to equations appropriate for flow through porous media. The flow equations consider relative permeability, gravitational effects, non-Darcy pressure drop, and non-Newtonian fluid rheology.

The fracture toughness is assumed to increase with the square root of fracture size. Experience has shown that scale-dependent toughness is critical to achieving realistic results. If the fracture toughness is assumed scale-independent, then either the toughness will be too low at late time (resulting in unrealistically long fractures) or too high at early time (resulting in unrealistically high injection pressures at the start of injection). McClure and Kang (2018) provide a literature review and discussion of this topic.

Perforation pressure drop is calculated at each cluster using Bernoulli's law (Cramer, 1987). It is proportional to the square of flow rate, and inversely proportional to the square of the number of shots and the fourth power of diameter. Perforation erosion is a function of proppant velocity through the perforations.

It is assumed that some proppant is trapped in the fracture and immobilized as it flows through the fracture. This captures the effect of small-scale fracture nonlinearity and roughness, such as branches, ledges, etc., that are observed in core across studies (Gale et al., 2018). We have found that if proppant immobilization is not included in the model, [the model predicts that?] proppant often settles entirely to the bottom of the fracture, leaving the fracture unpropped near the wellbore. This leads to unrealistic results because it causes the productivity of each cluster to be highly dependent on whether or not proppant managed to pile up and be placed at the well. Incorporating proppant immobilization in the model allows proppant to be trapped near the well and across much of the fracture height, yielding results that align much more consistently with actual field observations. However, not all proppant is trapped, and a large percentage settles out to the bottom of the fracture and forms an immobile bed.

Fractures are assumed to propagate linearly in the direction of SHmax. This is consistent with core across studies in the Wolfcamp and Eagle Ford, which observed that flow localized into subparallel hydraulic fractures striking in the direction of SHmax (Gale et al., 2018). Evidently, fracture turning is minimal in most shales because of sufficiently high horizontal stress anisotropy. While fracture geometry is certainly

complex at small scale, our approach is to perform field-scale planar fracture modeling, and then use constitutive equations (such as the proppant immobilization process described above) to handle the large-scale effects of small-scale processes below the resolution of the model.

Details of specific simulations

The geologic model was constructed from high-tier logs within the study area. Geomechanical properties were derived from dipole sonic logs with calibration to core and then used to determine the stress profile, using a normal pore pressure gradient. Parameters in the stress equation were calibrated with regional DFIT data from the study area. Petrophysical properties (porosity, water saturation, and permeability) were derived from log data, calibrated to core. From the calibrated log data, a layer-cake geologic model was constructed with regular gridding parallel to the well-axis, logarithmic gridding perpendicular to the well, and irregular, property-guided layering in the z-direction. The model well was landed in the middle of the Spraberry zone, to ensure that fractures and production would not be influenced by partial penetration of the higher permeability Jo Mill and Dean formations. Total system permeability and relative permeability were iteratively calibrated to achieve a gross match to typical production profiles from the Spraberry zone.

The model extends vertically 1000 ft. A layer cake model is used in which formation properties vary vertically but not laterally. This is a reasonable assumption because the formation is not structurally complex at the length scale of the model.

Figure 4 shows a perspective view of the 3D grid geometry, wellbore, and perforation clusters, with key initial properties populated into the grid. Figure 5 shows formation properties with respect to the landing depth and fracture geometry.

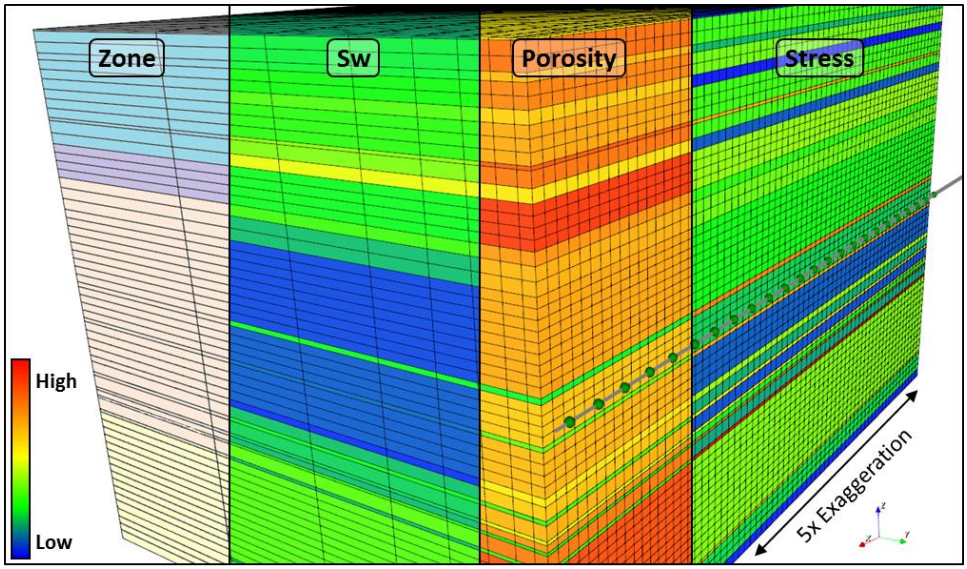

Figure 4. Geologic grid for hydraulic fracture and reservoir simulation.

Two sequential stages were pumped for each experimental stage design. Each slickwater stage included a small pad followed by 100 mesh and 40/70 mesh delivered with a continuous ramp from 0.5 PPA to 2.5 PPA. Injection rate was set to 50 BPM to reflect the lower rates resulting from the simul-frac operations. Pump schedules were customized for each design to deliver a consistent 1500 pounds of proppant per lateral foot of well length. The two stages were separated in time by 2 hours, with a 48 hour lag following the second stage to allow for proppant settling and closure, prior to production. Production for the two

stages was scaled to a equivalent maximum rate of 3500 bbl/10K ft lateral, constrained to a minimum bottom-hole producing pressure of 700 psi.

Flow simulations are performed for the two fracture stages with total production scaled up to a 10,000 ft lateral. No-flow boundaries are placed along the sides of the model perpendicular to the fractures to account for production interference from neighboring stages. The mesh length along fracture strike is 2200 ft, sufficiently long that the fractures do not propagate to the edge of the model. In reality, the well spacing is less than 1000 feet, but in the model, only one well is included. To account for production interference, the permeability of the rock farther than 500 ft from the well is set to zero after the well is placed on production.

Three different basic designs are compared, representing the evolution of completion design over 2018 (Table 2). Three major changes are apparent. First, stages are lengthening, requiring fewer stages to complete a typical lateral, resulting in time and cost savings. Second, cluster spacing is tightening in an effort to more effectively stimulate the low permeability reservoir. Third, perforation friction is increasing both through fewer shots per foot as well as smaller perforations in an effort to ensure that all perforation clusters are actively being stimulated. To demonstrate the need for limited-entry, an addition simulation was performed with Design 3 with more shots per foot and larger diameter perforations (Design 3b).

	DESIGN 1	**DESIGN 2**	**DESIGN 3**	**DESIGN 3b No LE**
Stage Geometry	125ft stages 6 clusters 21ft spacing	150ft stages 9 clusters 17ft spacing	165ft stages 12 clusters 14ft spacing	165ft stages 12 clusters 14ft spacing
Stages per 10K lateral	80	67	61	61
Perforations	4 spf 0.42”	2 spf 0.42”	2 spf 0.32”	6 spf 0.42”
BPM per perforation	2.1	2.8	2.1	0.7
Perforation friction	606 psi	1078 psi	1800 psi	67 psi
BPM per cluster	8.3	5.6	4.2	4.2
BPM per foot	0.40	0.33	0.30	0.30

Table 2. Alternative designs for hydraulic fracture modeling

Results and Discussion

Fracture geometry in the Design 1 simulation

Fracture geometry is controlled by the interplay of stress shadowing, perforation pressure drop (limited-entry), stress layering, fracture toughness, leakoff, viscous pressure drop along the fracture, and proppant transport. In this section, we discuss how these processes lead to the fracture geometries observed in the Design 1 simulation.

Figure 5, Figure 6, and Figure 8 show the fracture geometry from the Design 1 simulation. The fractures extend as far as 550 ft from the well, and up to 200 ft above and below the well landing depth.

Thin high stress layers above and below the landing zone create barriers to vertical fracture propagation. These barriers are thin carbonate debris flows, typically found within the Spraberry. As the fractures

open, they induce stress shadow on their neighbors, causing stress to build up. Because of the stress shadow, some of the fractures propagate upward and downward through the barriers.

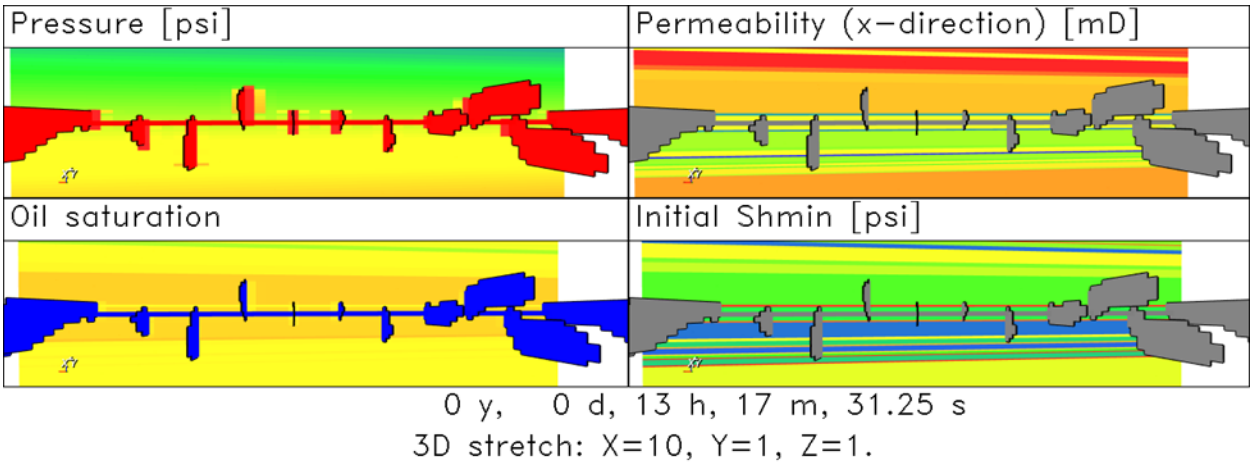

Figure 5: Fracture geometry with respect to formation layering in the Design 1 simulation. To aid visibility, the axis perpendicular to the fractures is stretched by 10x.

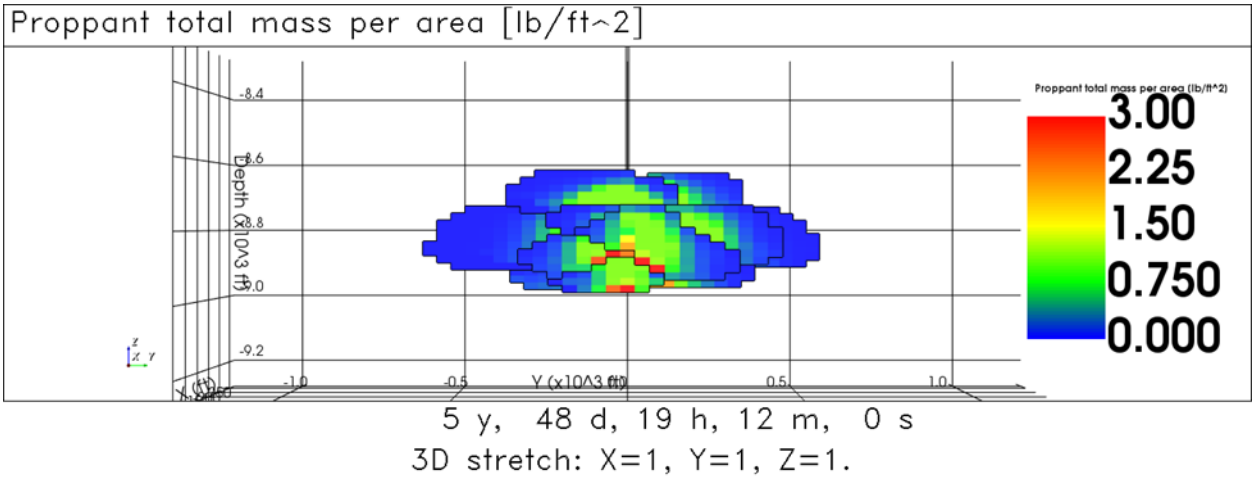

Figure 6: Fracture length and height from the Design 1 simulation.

Stress shadowing tries to localize stimulation into only a few fractures (i.e., cause poor perforation efficiency). Limited-entry combats this effect. Perforation pressure drop scales with the square of flow rate, and so it is minimized when flow is more even between the clusters (Cramer, 1987).

The lower left panel Figure 7 shows the fluid pressure on either side of a perforation cluster during the first stage. The pressure difference across the cluster is about 500 psi. The upper left panel shows the distribution of flow across the six clusters during the first stage. After 30 minutes, the flow distribution has stabilized and is fairly uniform, varying between 6 and 9 bpm per cluster. The perforation pressure drop gradually weakens over time because of perforation erosion caused by the proppant (lower right panel of Figure 7).

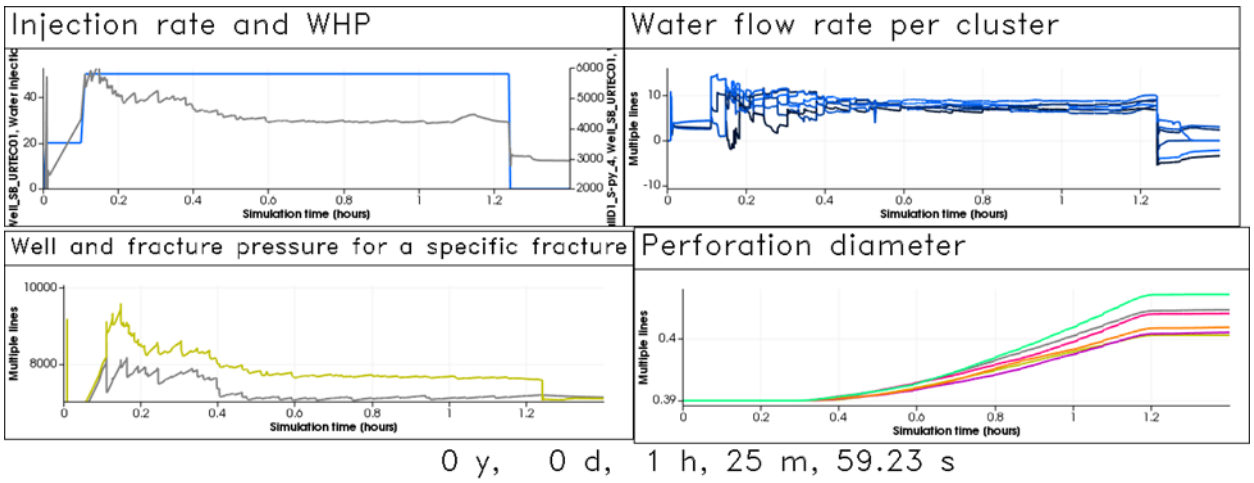

Figure 7: Parameters versus time during the first stage in the Design 1 simulation. Injection rate and WHP (upper left), net water flow rate per cluster (upper right), the fluid pressure on each side of the perforations (well and fracture) for a particular fracture (lower left), and perforation diameter (lower left).

Figure 8 shows the distribution of proppant, saturation, aperture, and pressure after 144 days of production. The fracture geometry is not symmetrical. The asymmetry develops as the fractures seek to minimize stress shadowing and avoid the shadow from their neighbors. The fractures extend up to 550 ft from the injection well.

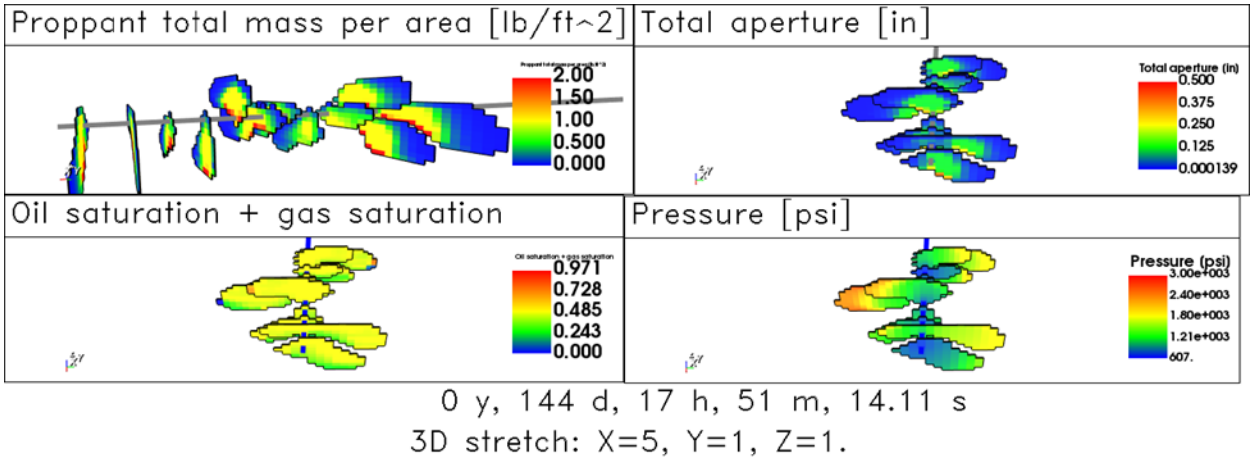

Figure 8: Distribution of proppant, saturation, aperture, and pressure after 144 days in the Design 1 simulation.

Because leakoff and viscous pressure gradient are low, the fracture length is limited by toughness. Proppant transport can influence fracture propagation if proppant screens out, either at the tip or at the perf clusters. In the Design 1 simulation, none of the clusters screened out, and so proppant transport did not have a dominant effect on fracture geometry. In the Design 3 simulation, the toe-most cluster screened out, as shown in Figure 16.

Processes impacting production

Figure 9 shows the distribution of proppant and conductivity in the fracture. During injection, proppant settles downward, forming accumulations along the bottom of the fractures. The proppant immobilization process allows a substantial volume of proppant to be trapped along the height of the fracture, creating good propped surface area. The proppant is able to flow hundreds of feet from the well, assisted by the rapid fluid flow rate, and the additional viscosity provided by the friction reducer.

Fracture conductivity is a strong function of proppant placement. In regions with substantial proppant placement, conductivity is on the order of 10s of md-ft. In regions without proppant, fracture conductivity is on the order of 0.1s of md-ft. Conductivity is a function of effective normal stress, and so these conductivities decrease over time as pressure is drawn down. The production calculation includes the effects of non-Darcy pressure drop, relative permeability, and non-Newtonian water viscosity during flowback (McClure and Kang, 2018).

Even though the conductivity is reasonably high, the fractures are not infinite conductivity. Because of the finite conductivity, several thousand psi of pressure gradient develops along the fractures due to flow (Figure 8 and Figure 9).

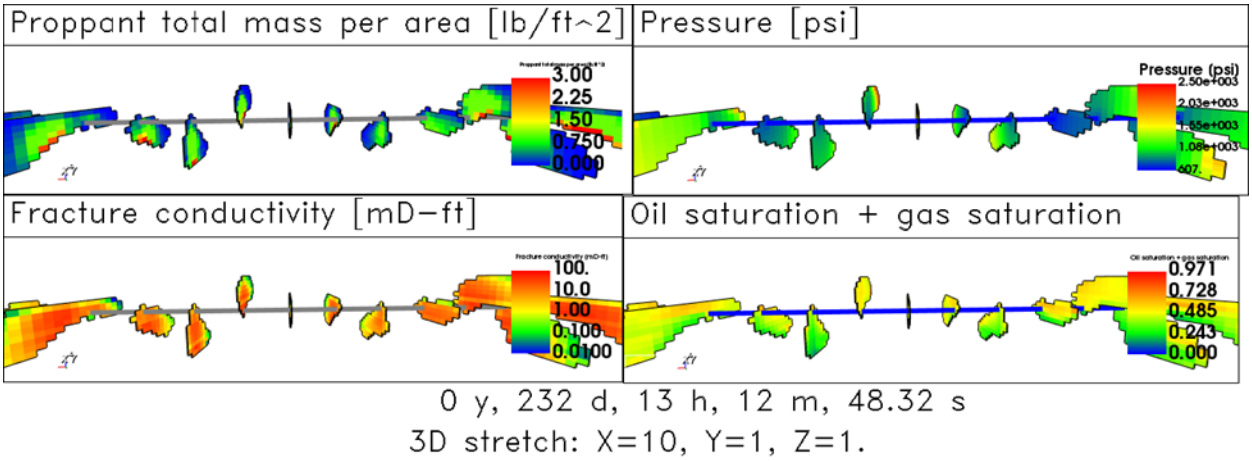

Figure 9: Distribution of proppant, conductivity, pressure, and saturation after 232 days in the Design 1 simulation. To aid visibility, the axis perpendicular to the fractures is stretched by 10x.

Figure 10 and Figure 11 show the distribution of fluid pressure and poroelastic stress change in the matrix after 144 days and five years. The grey regions of the matrix are the areas where permeability has been set to zero to account for pressure production interference from neighboring wells. Even after five years, large regions of the formation remain near initial pressure. Recovery is negatively affected by the asymmetric and uneven fracture growth. This leads to regions of the formation remaining undrained.

Pressure support is provided by solution gas drive as the fluid goes below the bubble point at 2517 psi. Figure 12 shows that substantial gas saturation develops in the fractures and in the regions of the formation near the fractures.

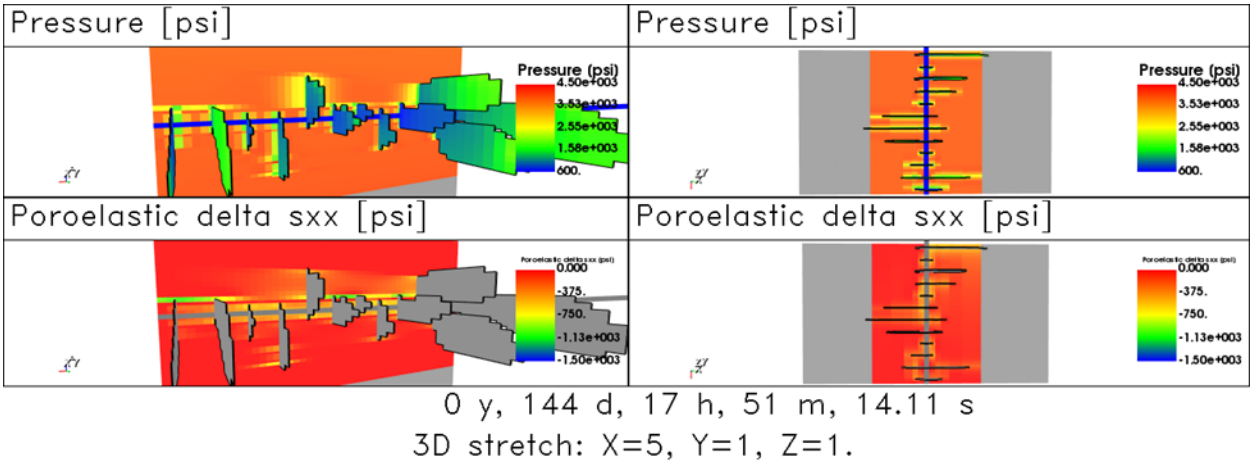

Figure 10: Distribution of pressure and poroelastic pressure change in the fractures after 144 days in the Design 1 simulation.

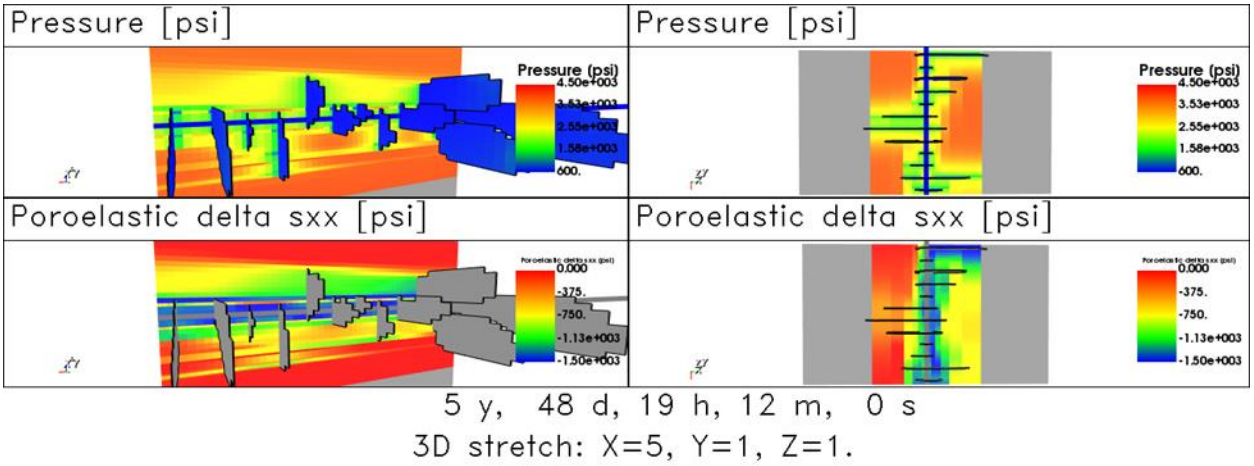

Figure 11: Distribution of pressure and poroelastic pressure change in the fractures after five years in the Design 1 simulation.

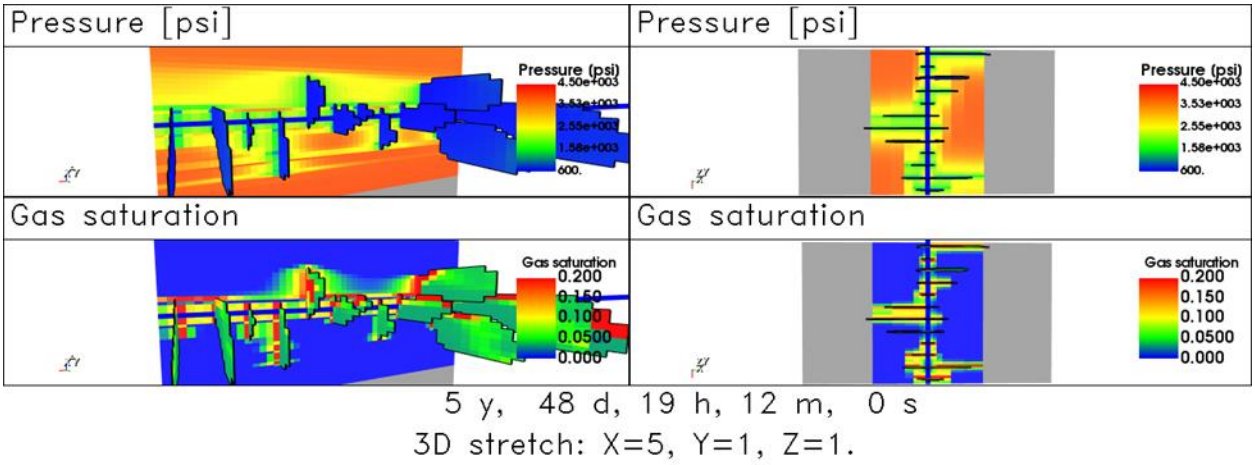

Figure 12: Distribution of pressure and gas saturation after five years of production in the Design 1 simulation.

Comparison of Designs 1-3

Figure 13 compares oil production per foot of lateral for the three designs, plus the Design 3b simulation withoutlimited-entry. Figure 14 and Figure 15 show the distribution of fluid pressure and poroelastic stress change in the Design 2 and Design 3 simulations.

Design 1 uses the widest cluster spacing, and Design 3 uses the tightest cluster spacing. All designs use similar water and proppant per ft, but the stage length increases from Design 1 to Design 3, lowering cost. Figure 13 shows that continuous improvement with tighter cluster spacing; Design 3 has the highest production, and Design 1 has the lowest production. Design 3 performs best even though it has lower cost because of tighter cluster spacing.

In order to maintain good cluster efficiency, the perforation design is modified to increase limited-entry from Design 1 to 3. Figure 16 shows that perforation pressure drop varies from 1000-2000 psi. Perforation erosion is more substantial in Design 3 than in Design 1 (Figure 7) because the smaller perforation diameter results in a higher linear velocity through the clusters.

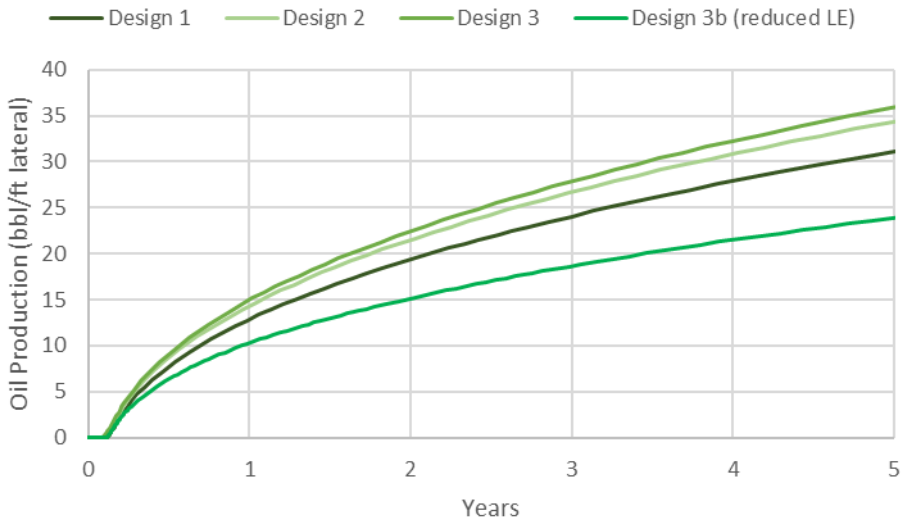

Figure 13: Oil production per foot for the three alternative designs

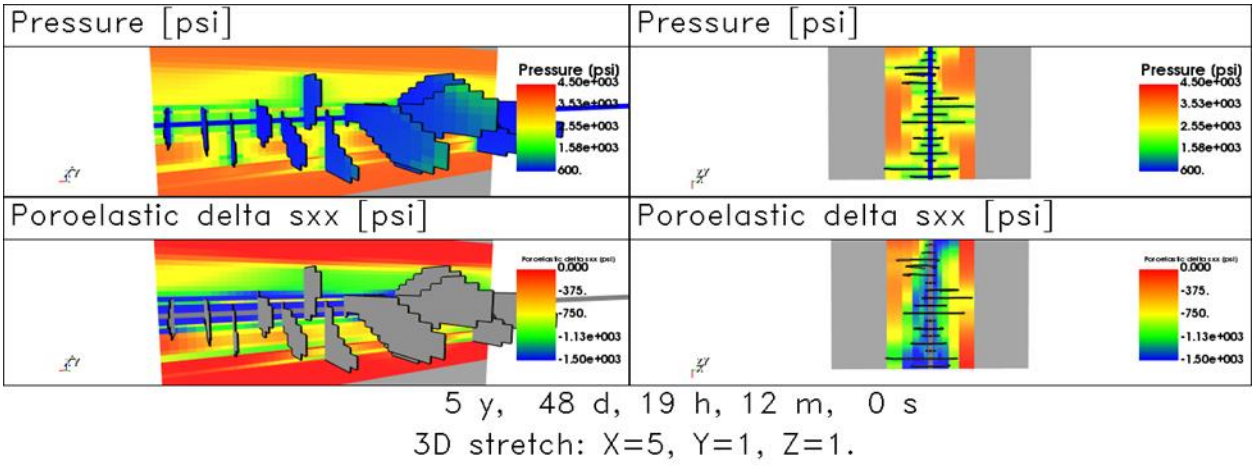

Figure 14: Distribution of pressure and poroelastic stress change in the Design 2 simulation.

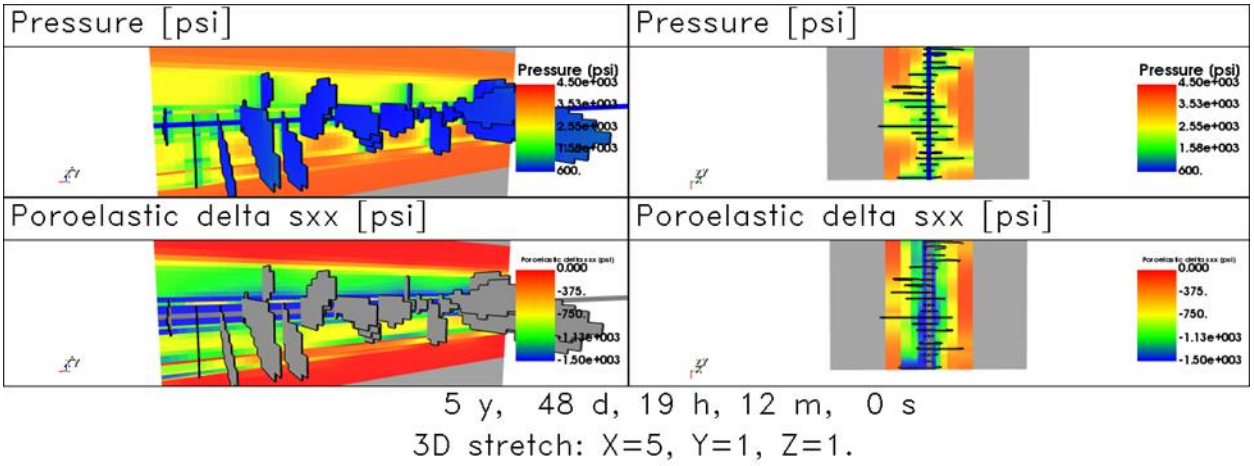

Figure 15: Distribution of pressure and poroelastic stress change in the Design 3 simulation.

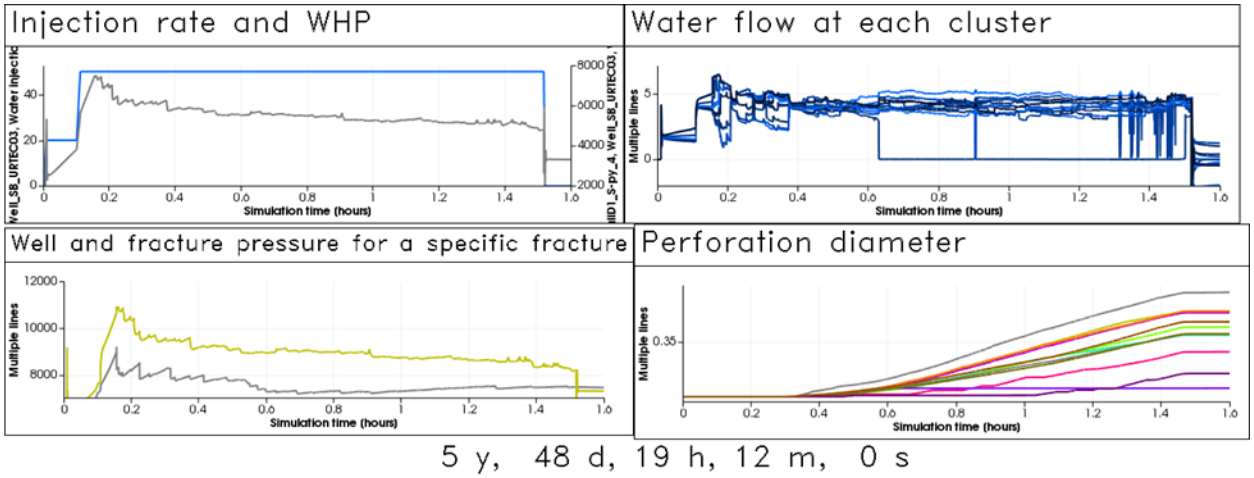

Figure 16: Parameters versus time during the first stage in the Design 3 simulation. Injection rate and WHP (upper left), net water flow rate per cluster (upper right), the fluid pressure on each side of the perforations (well and fracture) for a particular fracture (lower left), and perforation diameter (lower left).

In general, the optimal cluster spacing for production is determined by the interplay of perforation pressure drop, fracture geometry, fracture conductivity, fracture length, and well spacing. There is a tradeoff between minimizing production and stress shadow interference between fractures (by increasing spacing) and maximizing drawdown (by decreasing spacing).

If the fracture conductivity and well spacing were infinite, it would be optimal to create a single very long fracture per stage because this would minimize production interference between adjacent fractures. However, in practice, the benefit of fracture length is limited by pressure gradient along the fracture and by production interference from neighboring wells.

Production occurs through primary depletion and is driven by the pressure difference between the fracture and the formation. Near the well, where fluid pressure in the fracture is lower (because of finite fracture conductivity), there is more pressure differential to pull fluid in from the formation, resulting in greater production per area.

Tightening cluster spacing, while holding fluid and proppant per foot constant, causes roughly the same amount of propped fracture area to be generated, but causes more of that fracture area to be located near the well.

Tightening spacing does not have uniformly positive effects. Tightening spacing accelerates the onset of production interference between adjacent fractures. However, because some fractures grow up and down out of zone and growth is asymmetric laterally, the effective fracture spacing is often greater than the cluster spacing. For example, only a few fractures propagate up through the upper stress barrier (Figure 12). These fractures drain from the overlying zone with a much greater effective spacing than the cluster spacing.

In general, tightening spacing may decrease fracture length because it distributes the same amount of fluid into a larger number of fractures. Shorter fracture length has the potential to decrease long-term production. However, proppant cannot be transported an unlimited distance from the well, and so there is little benefit from propagating fractures further than the distance that proppant can be carried away from the wellbore. In many cases, the value of fracture length may also be limited by production interference from neighboring wells.

Value of limited-entry design

To illustrate the value of limited-entry, the Design 3 simulation was repeated without limited-entry in Design 3b: 6 shots per cluster with diameter of 0.42'' (instead of 2 shots at 0.32''). Figure 13 shows that the resulting production is significantly lower. Figure 17 and Figure 18 show the resulting fracture geometry, proppant placement, and depletion. Figure 19 shows the distribution of flow between the clusters and other injection parameters.

Without limited-entry, stress shadowing is able to inhibit propagation from most of the clusters. This comparison shows that tightening cluster spacing is valuable only if it is performed in conjunction with effective limited-entry.

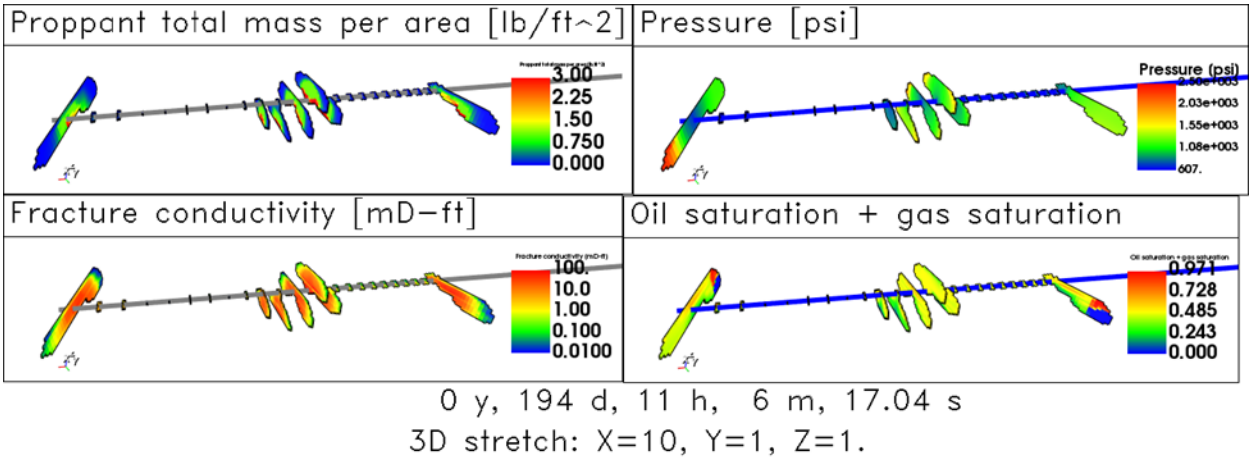

Figure 17: Distribution of proppant, conductivity, pressure, and saturation after 232 days in the Design 3b (no limited-entry) simulation. To aid visibility, the axis perpendicular to the fractures is stretched by 10x.

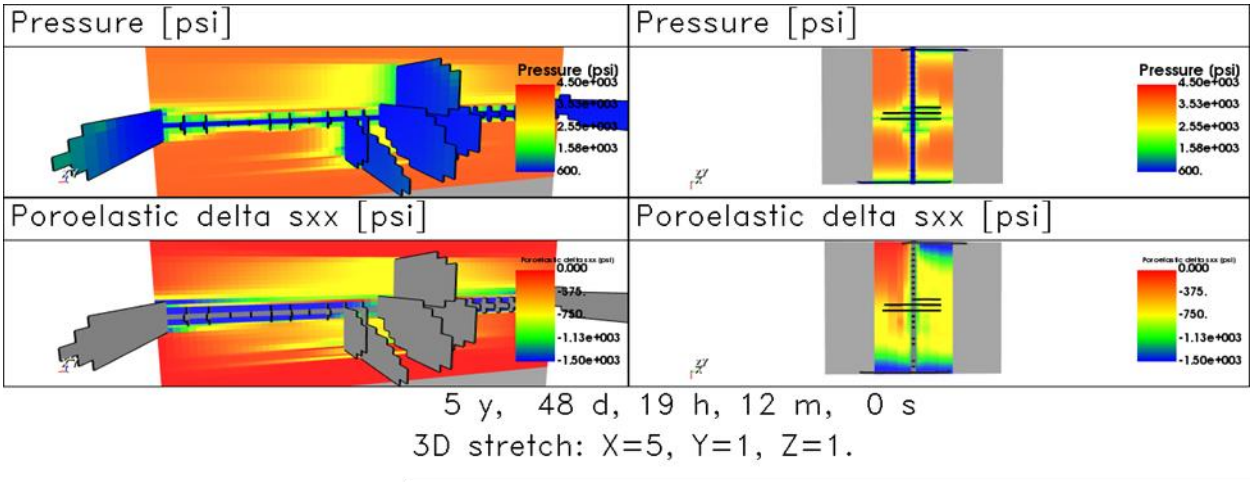

Figure 18: Distribution of proppant, conductivity, pressure, and saturation after 232 days in the Design 3b (no limited-entry) simulation. To aid visibility, the axis perpendicular to the fractures is stretched by 10x.

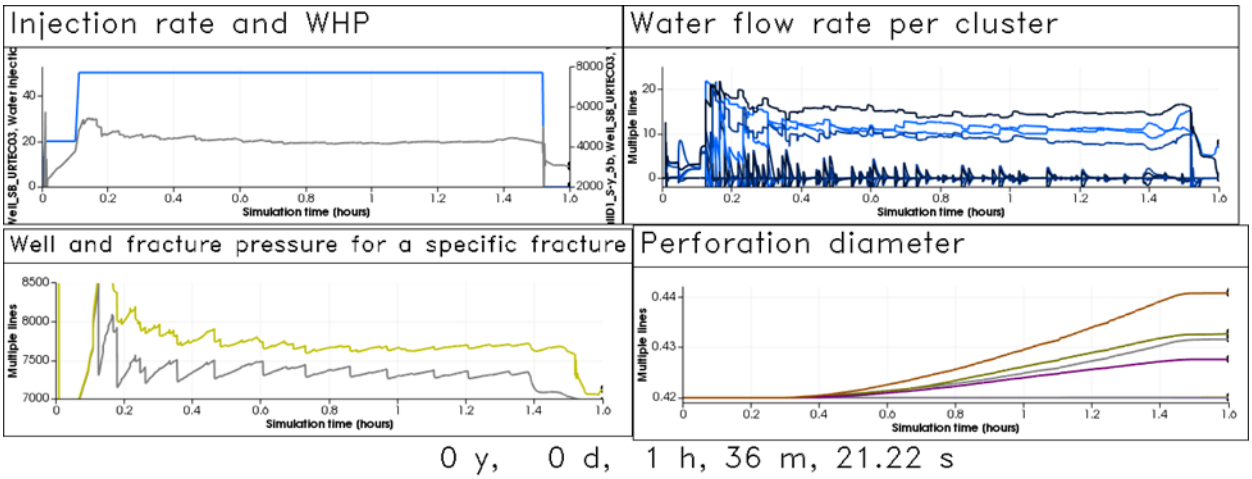

Figure 19: Distribution of proppant, conductivity, pressure, and saturation after 232 days in the Design 3b (no limited-entry) simulation. To aid visibility, the axis perpendicular to the fractures is stretched by 10x.

Conclusions

The simulations work hand-in-hand with continuous operational improvement. They demonstrate how production can be increased while simultaneously reducing cost. Reducing cluster spacing is valuable because of finite fracture conductivity. It is critical to increase perforation pressure drop in conjunction with reducing cluster spacing in order to maintain cluster efficiency.

Because production is controlled by a complex interplay of fracturing and reservoir processes, it is extremely valuable to describe the entire process with a single integrated fracturing and reservoir model. Optimal cluster spacing, limited-entry, and other design choices must be made for every formation (or even every well, if data is available) as part of a more comprehensive optimization of fracture design and field development planning.

Acknowledgements

We would like to thank QEP management for the opportunity to share this study with the industry. We would also like to thank Jill Thompson and Carrie Harrington for their contribution to this paper.

References

Cramer, D.D. 1987. The Application of Limited-Entry Techniques in Massive Hydraulic Fracturing Treatments. SPE 16189-MS presented at the SPE Production Operations Symposium, Oklahoma City, 8-10 March. http://dx.doi.org/10.2118/16189-MS

Gale, J. F., Elliott, S.J., and Laubach, S.E., 2018. Hydraulic Fractures in Core from Stimulated Reservoirs: Core Fracture Description of HFTS Slant Core, Midland Basin, West Texas, Presented at URTeC Conference, Houston, Texas, 23-25 July. URTEC-2902624-MS. https://doi.org/10.15530/URTEC-2018-2902624.

McClure, M., and Kang, C., 2018. ResFrac Technical Writeup, https://arxiv.org/abs/1804.02092.

Thompson, J., Franciose, N., Schutt, M., Hartig, K. and McKenna, J., 2018, Tank Development in the Midland Basin, Texas: A Case Study of Super-Charging a Reservoir to Optimize Production and Increase Horizontal Well Densities, presented at URTeC Conference, Houston, Texas, 23-25 July. URTEC-2902895-MS. http://doi.org/10.15530/URTEC-2018-2902895

Weddle, P., Griffin, L., and Pearson, C. M., 2018, Mining the Bakken II - Pushing the Envelope with Extreme Limited Entry Perforating. SPE Hydraulic Fracturing Technology Conference, The Woodlands, 23-25 January. http://doi.org/10.2118/189880-MS